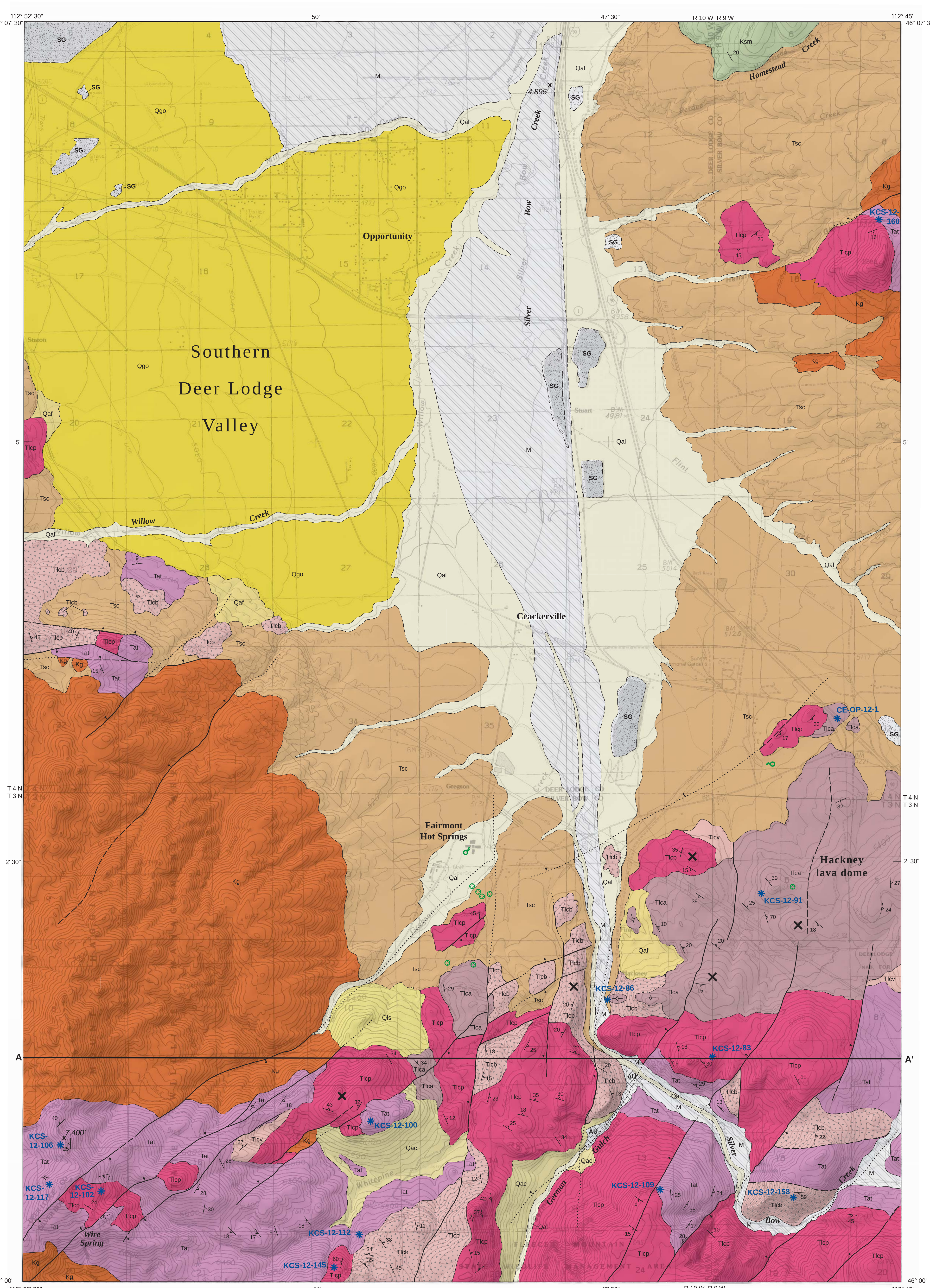

Base map produced by the United States Geological Survey
Control by: USGS, NOS/NOAA and USFS
Compiled from aerial photographs taken 1986
Field checked: 1987
Map edited: 1989
Projection: Lambert Conformal Conic
Grid:1000 meter Universal Transverse Mercator Zone 12
UTM grid declination: 1° 18' East
1989 Magnetic NorthDeclination: 16° 30' East
Vertical Datum: National Geodetic Vertical Datum of 1929
Horizontal Datum: 1927 North American Datum

N

SCALE 1:24,000
1 MILE
7000 FEET
1 KILOMETER
CONTOUR INTERVAL 40 FEET
NATIONAL GEODETIC VERTICAL DATUM OF 1929

Maps may be obtained from:
Publications Office
Montana Bureau of Mines and Geology
1300 West Park Street, Butte, Montana 59701-8997
Phone: (406) 496-4167; Fax: (406) 496-4451
http://www.mbmg.mtech.edu

Cross Section A–A'

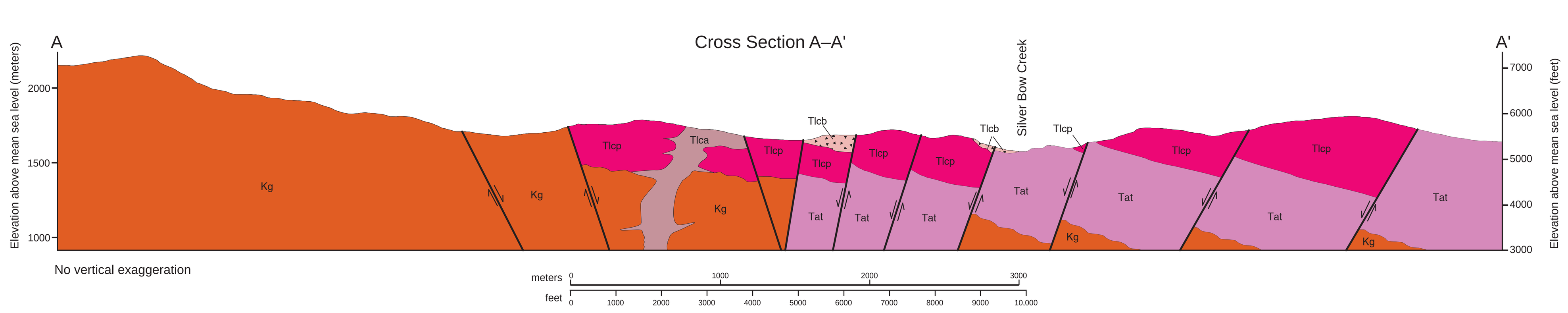

Research supported by the U.S. Geological Survey, National Cooperative Geologic Mapping Program, under USGS award number G12AC20277.
GIS production: Ken Sandau and Paul Thale, MBMG. Map layout: Susan Smith, MBMG.

CORRELATION DIAGRAM

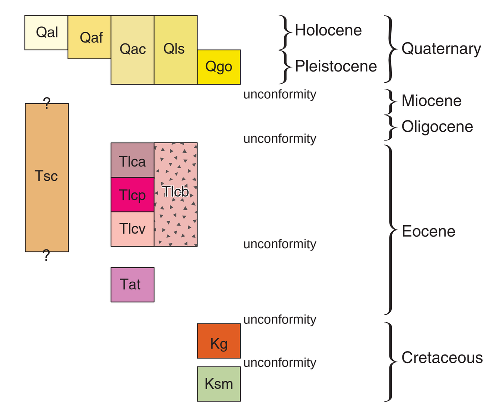

MAP SYMBOLS

Contact: dashed where approximately located

Fault: dashed where approximately located, dotted where concealed, bar and ball on downthrown side

Strike and dip of eutaxitic foliation

Vertically oriented eutaxitic foliation

Inactive volcanic vent

Geothermal spring and flow direction

Geothermal well

KCS-12-145 Sample location (Table 1)

INTRODUCTION

The Opportunity 7.5' quadrangle is located between Butte and Anaconda along the I-90 corridor in southwestern Montana (fig. 1). Silver Bow Creek, headwaters of the Clark Fork River (fig. 1), flows into the quadrangle from the east and then north into the Deer Lodge Valley. The elevation ranges by ~2,500' between the topographic high of 7,400' in the southwest part of the quadrangle to 4,895' along Silver Bow Creek in the north part of the quadrangle.

PREVIOUS MAPPING

Previous geologic studies in the quadrangle (fig. 1) include a 1:25,000 scale map by Noel (1956); a 1:50,000 scale map of the Deer Lodge Valley (Berg and Hargrave, 2004); and a geologic hazards assessment with 1:48,000 scale mapping of Silver Bow County (Elliott and McDonald, 2009).

GEOLOGIC SUMMARY

The bedrock geology features the contact between Late Cretaceous granite of the Boulder Batholith (Kg) and Eocene volcanic rocks of the Lowland Creek Volcanics (LCV) (Smedes and Thomas, 1965). The LCV formed in the hanging wall of the Anaconda Metamorphic Core Complex during the onset of east-directed detachment faulting (fig. 1) starting at 53 Ma (O'Neill and others, 2004; Dudas and others, 2010). The LCV are 1,830 m thick regionally and record at least one caldera-forming eruption cycle (Foster, 1987; Dudas and others, 2010). In the Opportunity 7.5' quadrangle the LCV are 800 m thick and consist of near vent andesite-rhyodacite lavas and pyroclastic deposits (fig. 2a, b, e, f, g) that overlie rhyolite ash (fig. 2h). The rocks record three stages of vulcanism.

1. The first stage (Tat) deposited 400 m of rhyolite (SiO_2 = 70.4–74.0 wt. percent; fig. 3, table 1) ash (fig. 2h), lithic-rich air-fall tuff, breccia, and poor-to-densely welded ignimbrite. The rhyolite deposits formed during several small eruptive pulses that culminated in a large ignimbrite eruption. $^{40}Ar–^{39}Ar$ analysis of biotite from a Tat feeder dike rock (sample KCS-12-112, table 1 and on map) yielded a concordant plateau age of 52.64 ± 0.39 Ma (fig. 4). $^{40}Ar–^{39}Ar$ analysis of biotite from welded ignimbrite (sample KCS-12-100, table 1 and on map) produced a concordant plateau age of 52.95 ± 0.45 Ma and analysis of plagioclase from the same rock yielded a concordant plateau age of 52.50 ± 0.32 Ma (fig. 4). The plateau age from plagioclase is statistically better than the biotite, which has a thermally disturbed degassing pattern in early heating steps (fig. 4). Tat correlates with the "lower tuff" of Smedes (1962), which crystallized at 52.9 ± 0.14 Ma ($^{40}Ar–^{39}Ar$ on biotite) (Dudas and others, 2010).

2. The second stage (Tlcp) produced 200 m of rhyodacite lavas (SiO_2 = ~ 69.9–71.9 wt. percent; fig. 3, table 1), vitrophyre, and tuff. The rhyodacite lavas sit on top of pink block and ash deposits north of Silver Bow Creek in the southeastern map corner. The lavas have well-developed autoclastic flow bases and blocks of rhyodacite are entrained in a basal, pink and oxidized, ash matrix (fig. 3e). These observations suggest that the eruption began explosively in water-saturated conditions and transitioned to an effusive eruption. Lapilli beds (fig. 2f) occur at the top of the unit and are associated with inactive single vent volcanos (fig. 2g). Chalcedony bands are abundant and record late-stage fumarole activity. $^{40}Ar–^{39}Ar$ analysis of plagioclase from a glassy dike rock (sample KCS-12-83, table 1 and on map) yielded a concordant plateau age of 51.79 ± 0.51 Ma (fig. 4). This unit correlates with rhyodacite porphyry lavas that crystallized at 52.4 ± 0.16 Ma ($^{40}Ar–^{39}Ar$ on hornblende) (Dudas and others, 2010) and perhaps the "lower lavas" of Smedes (1962).

3. The final stage (Tlca) formed a 6 km^3 andesite-dacite (SiO_2 = 60.0–65.2 wt. percent; fig. 3, table 1) lava dome, named here the Hackney lava dome (fig. 2c), over a northeast-trending fissure (Scarberry and others, 2015). This event resulted in thermal disturbance of older rocks near the fissure (sample KCS-12-100 on map) and is likely the cause of the complex gas release pattern in step-heating experiments on the Tat biotite (fig. 4; sample KCS-12-100). Ridge-forming masses of silicified pyroclastic breccia (fig. 2a, b) are remnants of the eruptive fissure. Pillow lavas, oxidized ash-clay beds, and fissure breccia indicates that the dome erupted through a water column. Ash and clay beds that contain twig and leaf impressions are exposed near the margins of Hackney lava dome and represent paleosols occupied by bodies of shallow standing water. The leaves are identifiable as fern, probably Anemia, which is characteristic of middle Eocene Green River and Clarno shale (S.R. Manchester, written commun., 2013). This unit is correlated with dacite lavas that erupted at 49.33 ± 0.68 Ma ($^{40}Ar–^{39}Ar$ on plagioclase) (Dudas and others, 2010) and the "upper lavas" of Smedes (1962).

NATURAL RESOURCES

Fairmont (Gregson) Hot Springs is a geothermal system localized by valley-bounding structures (e.g., Sonderegger, 1984). Geothermal springs and wells follow the contact between Eocene LCV and Late Cretaceous Boulder Batholith (Kg) granite as it projects into the southern Deer Lodge Valley and is cut by several faults (see map). Spring water is 71° C at the resort and about 129° C in its subsurface reservoir (Metesh, 2000). Intersecting northeast- and north-striking fault zones allow deep (4.3 km), and slow, groundwater circulation, if a geothermal gradient of 30° C/Km is assumed.

The final stage of LCV activity (Tlca) was centered over a northeast-trending Eocene fissure. Evidence for the fissure throughout the LCV in the southern half of the quadrangle includes silicified breccia, dikes, and inactive volcanic vents. The fissure may be an interesting target for mineral exploration. X-ray diffraction scans identify cristobalite, tridymite, albite, and ferric phosphate material (could be Pb, V, or As phosphate) in silicified breccia deposits (J. Dilles, written comm., 2015). These minerals are associated with < 150–180°C hydrothermal alteration near or in volcanic vent fumaroles and hot springs, which are favorable settings for low-grade, high-tonnage Au mineralization (e.g., Silberman, 1982).

Placer gold was discovered at German Gulch near its confluence with Silver Bow Creek in 1864. Placer workings produced ~$5 million in gold, which occurs as native gold, a telluride, within chalcopyrite and pyrite (Lyden, 2005).

ANTHROPOGENIC UNITS

SG **Sand and gravel pits (Holocene)**—Small roadside quarries.

M **Modified (Holocene)**—Contaminated soil that has been reclaimed. In 1908 floodwater in Silver Bow Creek deposited toxic streamside mine tailings from Butte and Anaconda into the Deer Lodge Valley. The EPA designated the region a Superfund Site in 1983 and started reclamation of the 100-year flood plain in 1999. Reclamation continues today.

AU **Placer gravels (Holocene)**—Piles of rounded river cobbles stacked within and along the banks of the modern river channel in German Gulch.

DESCRIPTION OF MAP UNITS

Qal **Alluvium (Holocene)**—Well-sorted gravel, sand, silt, and clay along modern streams and flood plains. Thickness undetermined but generally less than ~10 m.

Qaf **Alluvial fan (Holocene)**—Outspread, gently sloping mass of alluvium deposited by streams that issue from narrow channels in regions characterized by an abrupt change in topography. Thickness undetermined.

Qac **Colluvium (Holocene)**—Loose cobbles and pebbles within poor to moderately developed soil profiles. Deposits occur at the foot of cliffs or hill slopes and the material, including talus and cliff debris, has experienced limited, chiefly gravitational transport. Thickness less than 3 m.

Qls **Landslide deposit (Holocene)**—Mass wasting deposits of clay- to boulder-size sediment that include rotated or slumped blocks of bedrock and surficial sediment, soils, and mudflow deposits. Thickness undetermined.

Qgo **Glacial outwash (Pleistocene)**—Moderately to well-sorted cobble gravel, sand, and silt deposited by meltwater streams in front of the terminal margin of an active glacier. Prominent outwash deposits at the mouth of Mill Creek consist primarily of Precambrian Belt rocks and intrusive igneous rocks (Berg and Hargrave, 2004). Thickness undetermined.

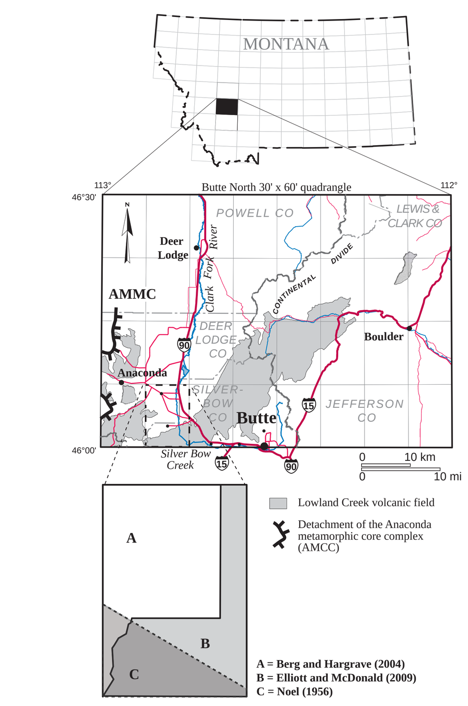

Figure 1. Location map shows Lowland Creek Volcanics and Anaconda Metamorphic Core Complex (AMCC) (after Vuke and others, 2007) and prior mapping in the Opportunity 7.5' quadrangle.

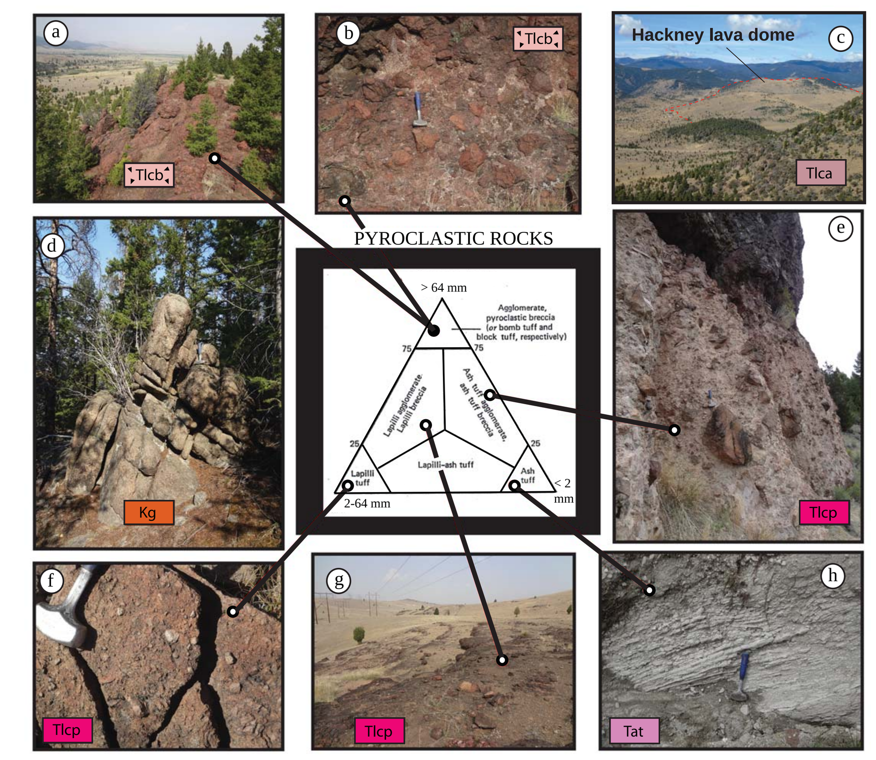

Figure 2. Field photographs highlight the diversity of pyroclastic deposits in the Opportunity 7.5' quadrangle.

Tsc **Six Mile Creek Formation (Miocene)**—Boulder and cobble gravel dominated by rounded to very well rounded quartzite clasts. Clasts are poorly- to well-sorted and up to 40 cm across. Mostly expressed as a lag deposit, though well-bedded boulder and cobble gravel is exposed in quarries around Crackerville (near center of map). The coarse gravel is interlayered with coarse to fine sand and silt which fines progressively towards the valley edges. Fine-grained deposits are weakly bedded mixtures of fluvial and debris flow material. Debris flows are unsorted masses with scattered coarse grains floating in a fine-grained matrix. Coarse sand and silt is locally derived from Boulder Batholith and Lowland Creek Volcanics. Poorly indurated and stratified beds of cobble and pebble conglomerate, and pale orange sand and silt form the moderately sloping benches on both sides of the southern Deer Lodge Valley. Colluvial benches of grus, well-rounded bedded quartzite cobbles, and boulders of granite and quartzite are 40 m thick south of Willow Creek (see map).

Lowland Creek Volcanics (Eocene)

Tlca **Lavas, hypabyssal intrusives, breccias, and phreatomagmatic deposits**—Black, fine-grained to aphanitic, glassy, and vesicular, andesite-dacite lavas, invasive lavas, hyalloclastite, and pillow lavas of the Hackney lava dome. The lower part consists of platy dikes and sills and massive cliff forming, silicified, red and black clast-supported breccia (fig. 2a, b). The intrusive facies exhibits < 1 mm phenocrysts of plagioclase, hornblende, and quartz. The uppermost part consists of red, green, and cream-colored patches of hyaloclastite (glass) and pillow lavas scattered amongst blocky, vesicular, aphanitic lava flows. The topographic limit of pillow lavas and hyaloclastites is ~645 m (5,400') in section 6, T. 3 N., R. 9 W. The composite thickness is ~120 m.

Tlcb **Volcanic breccia**—Deposits include silicified breccia within and marginal to the Hackney lava dome (Tlca), and mixed-texture breccia within the welded ash-flow tuff (Tat). All of the deposits are competent and generally monolithologic. Tlca breccia is highly silicified and formed during, and perhaps after, emplacement of the Hackney lava dome. Breccia associated with Tat exhibits a compositionally mixed texture between units Tlcp and Tat. This mixed-texture breccia may be part of a rhyolitic dike swarm located north of Silver Bow Creek.

Tlcp **Block and ash flows, vitrophyre, lavas, autobreccia, and lapilli tuff**—Coarsely porphyritic, compacted, ledge-forming dark gray-to-maroon rhyodacite outcrops that contain abundant plagioclase (commonly larger than 5 mm), biotite, hornblende and quartz phenocrysts set in a devitrified and oxidized groundmass. The base consists of 2–15 meters of salmon-pink block and ash tuff (fig. 2e). Lavas are locally vesicular and exhibit well-developed flow foliation at 2–10 cm spacing. An inactive vent complex (fig. 2g) with a footprint of 1.5 km^2 is centered in sec. 1, T. 3 N., R. 10 W. where 2 m of pink block and ash flows (fig. 2e) are overlain by porphyry lavas and lapilli tuff (fig. 2f). The entire 170-m thick section is exposed north of Silver Bow Creek in the SE ¼ sec. 12, T. 3 N., R. 10 W. where it overlies poorly consolidated ash-flow tuff (Tat).

Tlcv **Welded ash-flow tuff vitrophyre—**Black with a vitric to devitrified groundmass that typically contains abundant plagioclase phenocrysts. The vitrophyre is the glassy outer margin of dacite flows (Tlcp). The unit is <10 m thick and is typically exposed at or near the base of Tlcp.

Tat **Unconsolidated to welded, crystal-rich, air-fall and ash-flow tuff deposits**—Porphyritic gray rhyolite, welded ignimbrite, vapor-phase lithic-rich ignimbrite, stratified surge and air fall deposits, and white ashy lithic-bearing soils. The composite thickness approaches 400 m and consists of three discrete volcanic facies: (1) Spine-like outcrops of coarsely porphyritic welded ash-flow tuff and feeder dikes that are white, quartz-rich, coarse-grained with plagioclase phenocrysts up to 7 mm, and have steep inclined to sub-vertical eutaxitic foliation. Ridge-capping ignimbrite deposits, although similar in texture and appearance to the dikes, are locally crosscut by dikes and exhibit gently inclined eutaxitc foliation; (2) Lithic-bearing vapor-phase welded ignimbrite with vesiculated gas-escape horizons and abundant lithic clasts. The lithic clast assemblage consists of porphyritic maroon-purple volcanics, dark blue-black crystal-poor igneous rock, sandstone, granitic rock, white and tan chalcedony, and quartzite. Clast size increases up the section near Wire Spring in the southwestern corner of the quadrangle; (3) Nonwelded, pumice-bearing, lithic-rich air-fall and surge deposits (fig. 2h) characteristic of the basal deposits. Lithic pebbles-cobbles are poorly stratified and similar in composition to pebbles and cobbles within overlying lithic-rich welded tuff.

Boulder Batholith (Late Cretaceous)

Kg **Granitic rocks, undivided (Cretaceous)**—Coarse- and fine-grained, light to dark gray, pinkish and bluish gray intrusive rocks associated with the 74–78 Ma Boulder Batholith (Lund and others, 2002; du Bray and others, 2009; Elliott and McDonald, 2009). In the Opportunity quadrangle the rock is mostly the Butte Granite (Lund and others, 2002) (Figure 2, photo d); which has a modal mineralogy that includes normally zoned plagioclase (45–50 percent), orthoclase (20–30 percent), and quartz (5–10 percent) (Berg and Hargrave, 2004). The Butte Granite has an age of 76.28 ± 0.12 Ma (SHRIMP-RG U-Pb on zircon) (Martin and Dilles, 2000).

Ksm **Metamorphosed sedimentary rock (Cretaceous)**—Near the margins of the Boulder Batholith (Kg), the Blackleaf and Kootenai Formations are metamorphosed to hornfels, quartzite and marble (Elliott and McDonald, 2009). The unit is exposed north of Homestead Creek, in the northeastern map corner. T he exposed thickness is 75 m.

Table 1. Major and trace element data for samples of the Lowland Creek Volcanics collected in the quadrangle. Sample # corresponds to the sample location on the map. Sample ID is used on $^{40}Ar–^{39}Ar$ age spectra diagrams (fig. 4).

sample ID	KCS-12-158	KCS-12-117	KCS-12-100	KCS-12-112	KCS-12-102	KCS-12-109	KCS-12-106	KCS-12-160	KCS-12-83	KCS-12-145	KCS-12-91	CE-OP-12-1	KCS-12-86
map unit	Tlcb	Tat (w)	Tat (w)	Tat (w)	Tat (w)	Tat (w)	Tat (lt)	Tlcp (w)	Tlcp (d)	Tlcp (w)	Tlca (l)	Tlca (l)	Tlca (d)
XRF (wt. %)													
SiO_2	74.67	73.95	73.80	72.71	72.24	71.50	70.41	71.94	71.28	69.84	65.15	62.59	60.01
TiO_2	0.32	0.25	0.25	0.39	0.26	0.34	0.34	0.24	0.36	0.44	0.71	0.90	1.09
Al_2O_3	13.66	13.96	14.09	13.83	15.02	15.58	15.59	15.07	15.19	15.44	15.92	16.20	16.03
$^{*}FeO_T$	1.82	1.59	1.56	2.53	1.83	1.79	2.23	1.68	2.11	2.86	4.40	5.68	6.43
MnO	0.01	0.04	0.02	0.03	0.02	0.02	0.04	0.03	0.02	0.02	0.06	0.07	0.09
MgO	0.25	0.83	0.83	1.14	0.77	0.67	1.18	1.01	0.60	1.12	2.70	2.89	4.23
CaO	1.64	1.98	1.89	2.82	1.91	2.05	2.94	2.29	1.98	3.06	4.07	4.85	5.71
Na_2O	3.78	3.85	3.82	3.36	3.97	4.12	4.17	4.13	4.29	3.91	3.81	4.07	4.02
K_2O	3.73	3.48	3.64	3.07	3.93	3.84	2.99	3.53	4.04	3.16	2.99	2.56	2.12
P_2O_5	0.11	0.08	0.08	0.11	0.07	0.08	0.10	0.08	0.12	0.14	0.20	0.21	0.27
LOI	1.29	0.77	1.92	2.08	0.93	1.15	0.96	0.41	0.51	1.96	1.41	1.70	0.82
a.t.	98.90	98.84	98.57	97.50	98.70	98.75	98.39	99.45	99.63	97.78	98.40	98.59	99.48
Trace elements (ppm) (XRF)													
Ni	22	18	37	22	19	13	34	22	19	40	66	111	114
Cr	35	44	96	47	40	34	87	47	34	108	132	159	179
Sc	6	5	11	7	6	8	10	8	6	11	17	19	22
V	40	35	55	37	36	39	50	37	33	62	106	127	158
Ba	1302	1235	1067	1558	1331	1373	1266	1290	1307	1123	1480	1172	1125
Rb	131	120	84	142	127	129	89	107	123	94	87	82	54
Sr	509	627	660	592	638	628	847	777	618	731	830	705	882
Zr	229	135	155	262	143	190	148	137	134	178	284	256	277
Y	10	11	13	13	11	12	12	12	19	15	20	42	20
Nb	24	12	10	26	15	13	10	9	13	12	21	18	18
Ga	27	26	24	31	29	30	26	27	27	26	30	28	27
Cu	15	5	16	6	7	13	10	6	5	14	30	65	26
Zn	85	51	74	39	66	102	70	54	54	77	103	130	109
Pb	27	30	21	31	32	28	21	27	32	21	19	13	10
La	50	24	25	61	20	38	25	26	37	30	63	56	51
Ce	92	45	43	109	39	57	50	43	46	48	116	92	106
Th	23	9	7	27	8	12	7	6	7	8	14	11	10
Nd	31	20	20	34	12	27	20	17	29	25	41	40	42
U	4	3	2	6	4	3	2	2	3	4	3	2	2

(XRF) = X-ray fluorescence, (LOI) = Loss on ignition, (a.t.) = analytical total. Analyses performed by staff at the Geoanalytical Laboratory at Washington State University.
*All Fe expressed as Fe^{+2}. (w) = welded, (lt) = lithic tuff, (d) = dike, (l) = lava

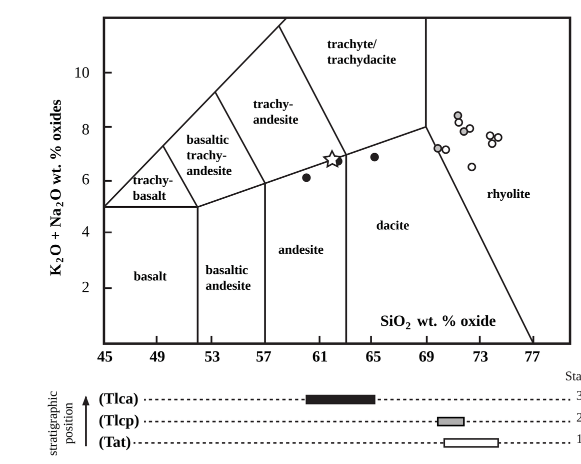

Figure 3. Rock type diagram shows the composition of Lowland Creek Volcanics samples collected in the Opportunity 7.5' quadrangle, after LeBas and others (1986). The star represents sample 93-15, analyzed by Dudas and others (2010). Note that the samples show compositional zoning of the deposits to lower silica content with time.

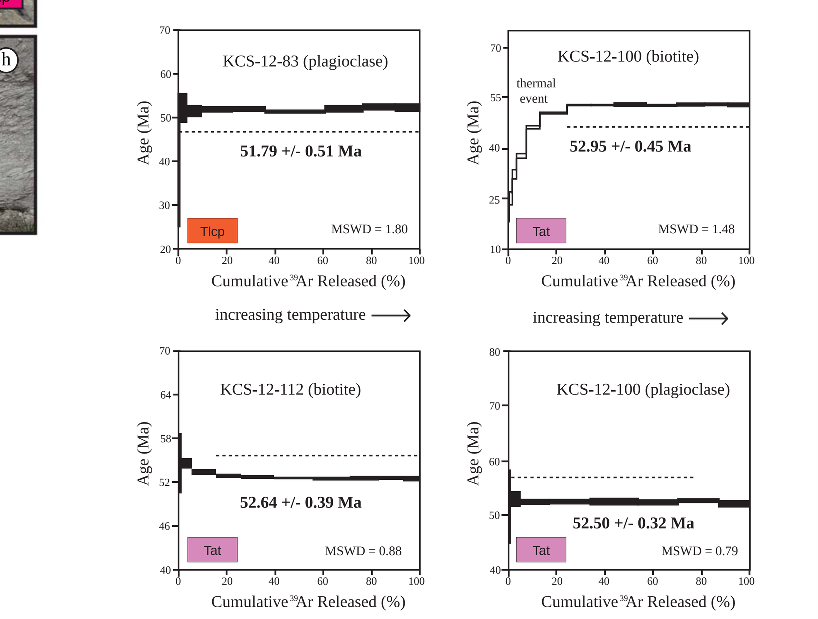

Figure 4. $^{40}Ar–^{39}Ar$ age spectra diagrams from step-heating experiments on samples of Lowland Creek Volcanics collected in the Opportunity 7.5' quadrangle. A weighted mean age is calculated from $^{40/39}Ar$ gas ratios measured at each step-heating experiment (black rectangles). Five concordant heating steps in which > 50% of ^{39}Ar is released defines an age plateau. The statistical robustness of the age plateau is quantified by the mean standard weighted deviance (MSWD) from each step used in the plateau. All samples produced age plateaus (dash line). KCS-12-100 (biotite) exhibits a complex gas release pattern. The apparent young ages in early heating steps is due to ^{39}Ar loss during a post-crystallization thermal event. Biotite is more susceptible to thermal affects than plagioclase (Hart, 1964). Experiments were conducted over a temperature range of 500–1400° C at Oregon State University

REFERENCES CITED

Berg, R.B. and Hargrave, P.A., 2004, Geologic map of the Upper Clark Fork Valley: Montana Bureau of Mines and Geology Open-File Report 506, 1:50,000 scale.
du Bray, E.A., Lund, K., Tilling, R.I., Denning, P.D., and DeWitt, E., 2009, Geochemical database for the Boulder batholith and its satellitic plutons, southwest Montana: U.S. Geological Survey Digital Data Series 454, 1 CD-ROM.
Dudas, F.O., Ispolatov, V.O., Harlan, S.S., and Snee, L.W., 2010, $^{40}Ar/^{39}Ar$ geochronology and geochemical reconnaissance of the Eocene Lowland Creek volcanic field, west-central Montana: Journal of Geology, v. 118, no. 3, p. 295–304.
Elliott, C.G. and McDonald, Catherine, 2009, Geologic map and geohazard assessment of Silver Bow County, Montana: Montana Bureau of Mines and Geology Open-File Report 585 (geologic map, 1: 50,000 scale).
Foster, Fess, 1987, Epithermal precious-metal systems associated with an Eocene cauldron: Lowland Creek volcanic field, southwestern Montana, *in* Berg, R.B. and Breuninger, R.H., eds., Guidebook of the Helena area, west-central Montana: Montana Bureau of Mines and Geology Special Publication 95, p. 53–54.
Hart, S.R., 1964, The petrology and isotopic-mineral age relations of a contact zone in the Front Ranges, Colorado: Journal of Geology, v. 72, p. 493–525.
LeBas, M.J., LeMaitre, R.W., Streckeisen, A., and Zanettin, B., 1986, A chemical classification of volcanic rocks based on the total alkali silica diagram: Journal of Petrology, v. 27, p. 745–750.
Lund, K., Aleinikoff , J.N., Kunk, M.J., Unruh, D.M., Zeihen, G.D., Hodges, W.C., du Bray, E.A., O'Neill, J.M., 2002, SHRIMP U-Pb and $^{40}Ar/^{39}Ar$ age constraints for relating plutonism and mineralization in the Boulder batholith region, Montana: Economic Geology v. 97, p. 241–267.
Lyden, C.J., 2013, Gold placers of Montana: Montana Bureau of Mines and Geology, Reprint 6, 120 p.
Martin, M. and Dilles, J., 2000, Timing and duration of the Butte porphyry system: Northwestern Geology, v. 25, p. 1.
Metesh, John, 2000, Geothermal springs and wells in Montana: Montana Bureau of Mines and Geology Open-File Report 415, 29 p., 2 appendices and state map.
Noel, J.A., 1956, The geology of the east end of the Anaconda Range and adjacent areas, Montana: Bloomington, Indiana University, Ph.D. dissertation, 74 p., (geologic map, 1: 25,000 scale)
O'Neill, J.M., Lonn, J.D., Lageson, D.R., and Kunk, M.J., 2004, Early Tertiary Anaconda metamorphic core complex: Canadian Journal of Earth Sciences, v. 41, p. 63–72.
Scarberry, K.C., Korzeb, S.L., and Smith, M.G., 2015, Origin of Eocene volcanic rocks at the south end of the Deer Lodge Valley, Montana: Northwest Geology, v. 44, p. 201–212.
Silberman, M.L., 1982, Hot-spring type, large tonnage, low-grade gold deposits, *in* Erickson, R.L., ed., Characteristics of Mineral Deposit Occurrences: U.S. Geological Survey Open-File Report 82-795, p. 131–142.
Smedes, H.W., 1962, Lowland Creek Volcanics, an upper Oligocene formation near Butte, Montana: The Journal of Geology, v. 70, no. 2, p. 255–266.
Smedes, H.W. and Thomas, H.H., 1965, Reassignment of the Lowland Creek Volcanics to Eocene age: Journal of Geology, v. 73, no. 3, p. 508–510.
Sonderegger, J.L., 1984, A summary of geothermal studies in Montana, 1980-1983: Montana Bureau of Mines and Geology Open-File Report 142, 45 p.
Vuke, S.M., Porter, K.W., Lonn, J.D., and Lopez, D.A., 2007, Geologic Map of Montana: Montana Bureau of Mines and Geology Map 62A, 1:500,000 scale.

Montana Bureau of Mines and Geology

MBMG Open-File Report 683

Geologic Map of the Opportunity 7.5' Quadrangle, Southwestern Montana

Kaleb C. Scarberry and Colleen G. Elliott

2016